

## Similitudes for the structural response and radiated sound power of simply supported plates

Olivier Robin<sup>\*1</sup>, Pasquale Margherita<sup>2a</sup>, Sergio De Rosa<sup>2b</sup>, Alain Berry<sup>1c</sup>, Francesco Franco<sup>2d</sup> and Elena Ciappi<sup>3e</sup>

<sup>1</sup>*Groupe d'Acoustique de l'Université de Sherbrooke, Faculté de Génie, Sherbrooke, J1K 2R1, Canada*

<sup>2</sup>*pasto-Lab, Department of Industrial Engineering, Università degli Studi di Napoli Federico II, Via Claudio 21, 80125 Napoli, Italy*

<sup>3</sup>*CNR-INM Institute of Marine Engineering, Via di Vallerano 139, 00128, Roma, Italy*

*(Received October 7, 2018, Revised March 23 2019, Accepted April 15, 2019)*

**Abstract.** This communication investigates exact and distorted similitudes and the related scaling laws for the analysis of both dynamic response and radiated power of rectangular plates. The response of a given panel in similitude from another one is determined from a generalization of the modal approach, allowing the use of mode shapes, natural frequencies and finally radiation functions in order to establish appropriate scaling laws. Analytical models of simply supported rectangular plates are used to produce both original and replica model responses under point mechanical excitation. Emphasis is then especially put on laboratory experiments which are performed on baffled simply supported aluminum panels under mechanical excitations. All the six possible scaling directions, *i.e.* predicting a plate vibroacoustic response from another plate, are reported. All obtained results show that structural response or radiated sound power of a given plate can be both recovered with satisfactory accuracy by using the related scaling laws, even if parent models are used.

**Keywords:** similitude; plates vibration; scaling

---

### 1. Introduction

The use of prototypes is often mandatory in many engineering fields and these prototypes should have dimensions that are convenient for laboratory testing, by either increasing or reducing the original ones, thus making very important to define possible similarity conditions or scaling laws. The similitude is considered a full branch of engineering science, especially

---

\*Corresponding author, Ph.D., Research associate, E-mail: [olivier.robin@usherbrooke.ca](mailto:olivier.robin@usherbrooke.ca)

<sup>a</sup>MSc, E-mail: [pasquale.margh@gmail.com](mailto:pasquale.margh@gmail.com)

<sup>b</sup>Professor, E-mail: [sergio.derosa@unina.it](mailto:sergio.derosa@unina.it)

<sup>c</sup>Professor, E-mail: [alain.berry@usherbrooke.ca](mailto:alain.berry@usherbrooke.ca)

<sup>d</sup>Professor, E-mail: [francesco.franco@unina.it](mailto:francesco.franco@unina.it)

<sup>e</sup>Researcher, E-mail: [elena.ciappi@cnr.it](mailto:elena.ciappi@cnr.it)

meant for the testing of models (*i.e.*, scaled ones). Main applications are found in aerospace engineering (1) or fluid mechanics (dimensionless numbers such as the Reynolds number is a typical scaling result). A recent review of reduced scale models can be found in (2).

In structural mechanics, similitude has been applied to several topics, and is typically well suited to the testing of down scaled elements (such as wind turbine blades before expensive and difficult full-scale testing (3)). When focusing to the more specific topic of shells or plates vibration, the problem of predicting the dynamic characteristics of such structures from those of their scale models has been investigated by several researchers (4, 5, 6, 7, 8, 9). The specific case of composite cylindrical shells vibration and their scaling was studied in (4). Other cited studies (5, 6, 7, 8, 9) focus on the scaling of vibration of rectangular plates, including plate assemblies (8) and distorted similitudes (9). The study proposed by (5) has the originality of introducing geometric, kinematic and dynamic similarities, so that scaling factors are proposed for length, natural frequency, but also time.

The previously cited studies are mostly restricted to numerical examples and never include the scaling of sound radiation. In this paper, the definition of scaling laws for studying both the structural response and radiated acoustic power of simply supported panels under point mechanical excitation is considered. This study relies on three panels with different length, width and thickness ratios. The effect of the scaling direction (*i.e.* from a panel with given dimensions to another one) is also studied, providing some concrete and hands-on considerations when a scaling procedure is considered. Emphasis is given to experimental validations that include both structural response and radiated sound power.

## 2. Theoretical background

### 2.1 General problem and similitude definitions

In what follows, the studied panels are considered thin, isotropic and have simply-supported boundary conditions. Since such boundary conditions lead to a simple and exact analytical solution to the plate equation of motion, theoretical investigations are simplified. Moreover, simply supported conditions can be achieved along all the plate boundaries using a dedicated method that has proved to be reliable (12). For such a plate of dimensions  $a \times b \times h$  (length per width per thickness), the mode shapes  $\phi_i$  and the natural frequencies (or eigenfrequencies)  $\omega_i$ , solutions of the free vibration equation, take simple closed-form expressions

$$\phi_i(x, y) = \sin\left(\frac{m_i\pi}{a}x\right) \sin\left(\frac{n_i\pi}{b}y\right), \quad (1)$$

$$\omega_i = \sqrt{\frac{Eh^2}{12\rho(1-\nu^2)}} \left[ \left(\frac{m_i\pi}{a}\right)^2 + \left(\frac{n_i\pi}{b}\right)^2 \right], \quad (2)$$

where  $E$ ,  $\nu$  and  $\rho$  denote the material Young's modulus, Poisson's ratio, and mass density, respectively, and  $m_i$  and  $n_i$  are non-zero strictly positive integers.

All plates will be considered mounted in an infinite rigid plane baffle (with a flow developing along the  $x$ -axis for the flow induced case). The plate lies in a  $x - y$  plane and the

flexural out-of-plane displacements,  $w(x, y, t)$ , are along the  $z$  axis.

In this paper, the derivation of the similitude laws is based on Refs. (8, 9). The symbol ( $\hat{\cdot}$ ) will always denote a parameter in similitude. Let us define a set of scaling parameters,  $r$ , as the ratios of the similitude parameter to the original one, for example:

$$r_x = \frac{\hat{a}}{a}; r_y = \frac{\hat{b}}{b}; r_h = \frac{\hat{h}}{h}; r_\eta = \frac{\hat{\eta}}{\eta}; r_\omega = \frac{\hat{\omega}_i}{\omega_i}; r_U = \frac{\hat{U}_c}{U_c}; r_p = \frac{\hat{S}_p}{S_p} \dots \tag{3}$$

They define the similitude ratios in terms of length ( $r_x$ ), width ( $r_y$ ), thickness ( $r_h$ ), structural damping ( $r_\eta$ ), angular frequency ( $r_\omega$ ), convective velocity ( $r_U$ ), single point spectral density of the excitation ( $r_p$ ), respectively. In all following developments, the material remains unchanged and the structural factor is supposed constant, *i.e.*  $r_\eta = \frac{\hat{\eta}}{\eta} = 1$ . For sake of simplicity, other damping sources (or mechanisms) are considered included in the term  $\eta$ . Also, the mode shapes  $\phi_i(x, y)$  (which describe the spatial dependence of both excitation and response points) will not need to be posed in similitude due to geometric scaling. They will include the dimensionless positions of the source and receiver points. Any variation of the geometry and/or the material will alter the distribution of the natural frequencies and it is assumed that the boundary conditions and the mode shapes are left unaltered. All the results presented hereinafter can be generalized to any panel type provided the conditions previously expressed are fulfilled, as was made for example in (9) for the case of panels with 'clamped-free-free-free' boundary conditions.

2.2 Similitude for flexural plates under point mechanical excitation

Some background on the theory behind the similitude using the modal approach is given here. The forced response in terms of vibration velocity of a given plate can be written as follows:

$$v(A, B; \omega) = j\omega\Lambda \sum_{i=1}^{N_M} \frac{\phi_i(A)\phi_i(B)}{[(\omega_i^2 - \omega^2) + j\eta_i\omega_i^2]} \tag{4}$$

This describes the generic output response at a point  $A(x_A, y_A)$  when the system is forced at a point  $B(x_B, y_B)$ ;  $i$  denotes the mode index associated with the  $i$ -th structural mode and  $\eta_i$  the structural loss factor.  $\Lambda$  represents the ratio of the force amplitude  $F$  over the generalized mass  $\mu_i$  and  $j = \sqrt{-1}$ .

A harmonic force  $f(B; t)$  is considered acting at a point  $B$  with a constant force amplitude  $F$ ,  $f(B; t) = F\delta(B_0 - B)e^{j\omega t}$ . The response of this system in similitude can be written as follows

$$\hat{v}(A, B; \omega) = j\omega r_\lambda \sum_{i=1}^{N_M} \frac{\phi_i(A)\phi_i(B)}{\left[ \left( \omega_i^2 - \left( \frac{\omega}{r_\omega} \right)^2 \right) + j\eta\omega_i^2 \right]} \tag{5}$$

According to the previous equation, the main condition to obtain an exact similitude is easily attributed to the distribution of natural frequency,  $r_\omega$ ,  $r_\Lambda$  being only a scaling

parameter. Looking for a distorted similitude implies searching scaling parameters which allow satisfying the following condition

$$v(A, B; \omega) \approx \hat{v}(A, B; r_\omega \omega; r_\Lambda \Lambda) \quad (6)$$

The velocity response in similitude will be for  $MN$  modes ( $M$  along  $a$  and  $N$  along  $b$ ):

$$\hat{v}(A, B; \omega) = \left( \frac{r_F}{r_x r_y r_h r_\omega} \right) \left( \frac{4jF}{\rho abh} \right) \left( \frac{\omega}{r_\omega} \right) \sum_{i=1}^{MN} \frac{\sin(m_i \pi \xi_A) \sin(n_i \pi \zeta_A) \sin(m_i \pi \xi_B) \sin(n_i \pi \zeta_B)}{\omega_i^2 - \left( \frac{\omega}{r_\omega} \right)^2 + j\eta \omega_i^2} \quad (7)$$

and finally

$$\hat{v}(A, B; r_\omega \omega) = \frac{r_F}{r_x r_y r_h r_\omega} v(A, B; \omega) = \frac{r_F}{r_{mass} r_\omega} v(A, B; \omega) \quad (8)$$

with  $r_{mass} = r_x r_y r_h$ . Symbols  $\xi$  and  $\zeta$  stand for dimensionless coordinates ( $\xi_{A,B} = \frac{x_{A,B}}{a}$ , and  $\zeta_{A,B} = \frac{y_{A,B}}{b}$ ).

The variations are geometrical, involving only  $r_x$ ,  $r_y$  and  $r_h$ , the scaling coefficients upon length, width and thickness. In this scheme  $r_F$  and  $r_{mass}$ , the ratio of the force amplitudes and of the generalized mass in similitude work as simple correction factors. The only condition to obtain an exact similitude is that the natural frequencies of the parent plate can be proportionally written with those of the original plate: (a)  $r_x = r_y = r_h$ : the similitude is denoted as *replica*; (b)  $r_x = r_y$  for any  $r_h$ : a *proportional side* similitude is obtained; (c)  $r_x \neq r_y$ : a distorted similitude (*avatar*) is obtained. The cases (a) and (b) are both exact similitudes. It can be shown that the unique choice for  $r_\omega$  is, in those cases,  $r_\omega = \frac{r_h}{r_x r_y}$ .

### 2.3 Radiated acoustic power under similitude

The radiated acoustic power  $\Pi$  from a plane radiator can be obtained by (13)

$$\Pi = \tilde{\mathbf{v}}^H \mathbf{R}_{rad} \tilde{\mathbf{v}} = Tr(\mathbf{S}_{\mathbf{v}\mathbf{v}} \mathbf{R}_{rad}), \quad (9)$$

where  $\tilde{\mathbf{v}}$  is the  $[N \times 1]$  vector of measured complex vibration velocities at  $N$  points on a regular grid on the panel,  $\mathbf{H}$  is the Hermitian transpose,  $\mathbf{S}_{\mathbf{v}\mathbf{v}}$  is the cross-spectral density matrix of vibration velocity and  $Tr$  is the trace of matrix. Finally,  $\mathbf{R}_{rad}$  is the element radiation matrix (13) of dimension  $[N \times N]$  for a baffled panel, which elements are defined as

$$R_{rad} = \frac{\omega^2 \rho_0 A^2 \sin(k_0 d)}{4\pi c_0 k_0 d}, \quad (10)$$

where  $k_0$  is the acoustic wavenumber,  $A$  is the elemental area of each measurement point and  $d$  is the distance from one element to another. Eqs. (9, 10) hold for any boundary conditions

of the panel, do not depend on the velocity distribution on the panel and finally assume that it is baffled and that the receiving space is anechoic.

Here, the radiation function has to be put into similitude, that is

$$\hat{R}_{rad}(\hat{\omega}, \hat{d}) = \frac{\hat{\omega}^2 \rho_0 \hat{A}^2 \sin(\hat{k}_0 \hat{d})}{4\pi c_0 \hat{k}_0 \hat{d}} = \frac{\hat{\omega}^2 \rho_0 \hat{A}^2 \sin(\frac{\hat{\omega}}{c_0} \hat{d})}{4\pi c_0 \frac{\hat{\omega}}{c_0} \hat{d}} = \frac{(r_\omega \omega)^2 \rho_0 \hat{A}^2 \sin(r_\omega r_d \frac{\omega}{c_0} d)}{4\pi c_0 r_\omega r_d \frac{\omega}{c_0} d} \quad (11)$$

The equality  $\hat{R}(\hat{\omega}, \hat{d}) = R(\omega, d)$  is obtained only if  $r_\omega r_d = 1$  (with  $r_d$  the ratio of the distance between elemental radiators between similitude and original panel -  $\hat{A}$  is directly related to  $A$  using  $r_x$  and  $r_y$  and a scaled point mesh). In this study, this condition is always assumed, thus working only with replicas and proportional type similitudes. The investigations on modification of the radiation operator with the related avatars are left to future works.

### 3. Description of plates considered in the study

Three plates are considered in this study, and their dimensions are reported in Table 1. The material properties are those of a typical aluminum alloy, with a Young's modulus value  $E = 70$  GPa, a mass density  $\rho = 2700$  kg.m<sup>-3</sup>, a Poisson's coefficient  $\nu = 0.3$  and a structural damping  $\eta = 0.02$  (considered constant as a function of frequency). The derived similitude ratios (or scaling coefficients) are also reported in Table 1. For the numerical part of this work, the vibroacoustic response of panels was analytically calculated following Section 2. Concerning the experimental validation, three panels were built following (12) to obtain representative simply supported boundary conditions.

For both numerical and experimental parts, the structural mesh and the excitation point coordinates are treated in similitude, so as to finally have dimensionless positions. For each test case, a mechanical excitation is applied at coordinates  $x = 0.4 a$  and  $y = 0.7 b$ .

In this study, the plate A is considered as the reference plate. This assumption is done only for sake of simplicity. Basically, each plate can be used as reference and the other plates can be considered as domains in similitude.

Table 1 Plate dimensions (mm) and corresponding scaling coefficients

Plate	$a$	$b$	$h$	$r_x$	$r_y$	$r_h$	$r_\omega$
<b>A</b> Reference	480	420	3.2	-	-	-	-
<b>B</b> Proportional Sides, same thickness	600	525	3.2	1.25	1.25	1.00	0.64
<b>C</b> Proportional Sides, ≠ thickness (replica)	240	210	1.6	0.5	0.5	0.5	2

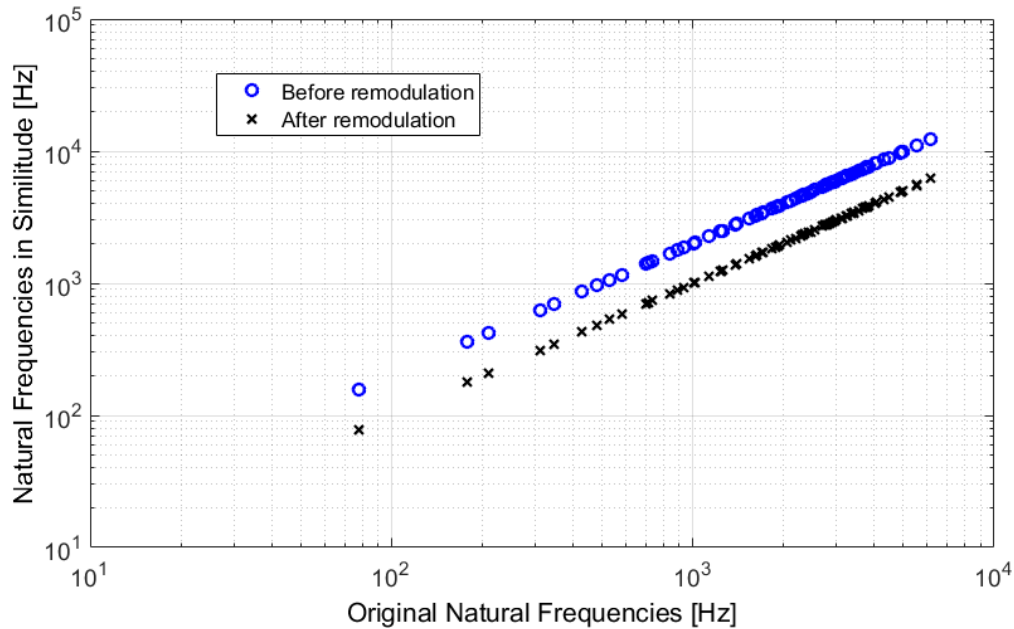


Fig. 1 Re-modulation of natural frequencies from panel C (before) to panel A (after).

#### 4. Numerical results

Figure 1 first shows the effect of re-modulating the natural frequencies using the ratio  $r_\omega$ , from panel C (before re-modulation) to panel A. With similar material and boundary conditions (and thus modal distribution), the frequency scaling is simply a translation in the domain of original to similitude natural frequencies.

The theoretical mobility (vibration velocity upon force) at the force injection point is shown in Figure 2 for the three considered plates on the 0 – 3000 Hz frequency range. The amplitude and frequency distributions are overall very different on the considered frequency range. The similitude laws defined in Section 2 are then used to recover the vibration response of the original plate (A) from the knowledge of the vibration response of the proportional sides plate (B) or the replica plate (C). The results of the scaling procedure in these two cases are given in the upper and lower parts of Fig. 3, respectively. The original and re-modulated responses perfectly overlap in the case of replica or proportional side plates, as already shown in several publications (8, 9, 14). The lower part of Fig. 3 highlights the fact that if the ratio  $r_\omega$  is larger than unity (as for plate C), the solution for the plate C should be developed up to 6000 Hz to scale the structural response for plate A in the whole considered frequency range.

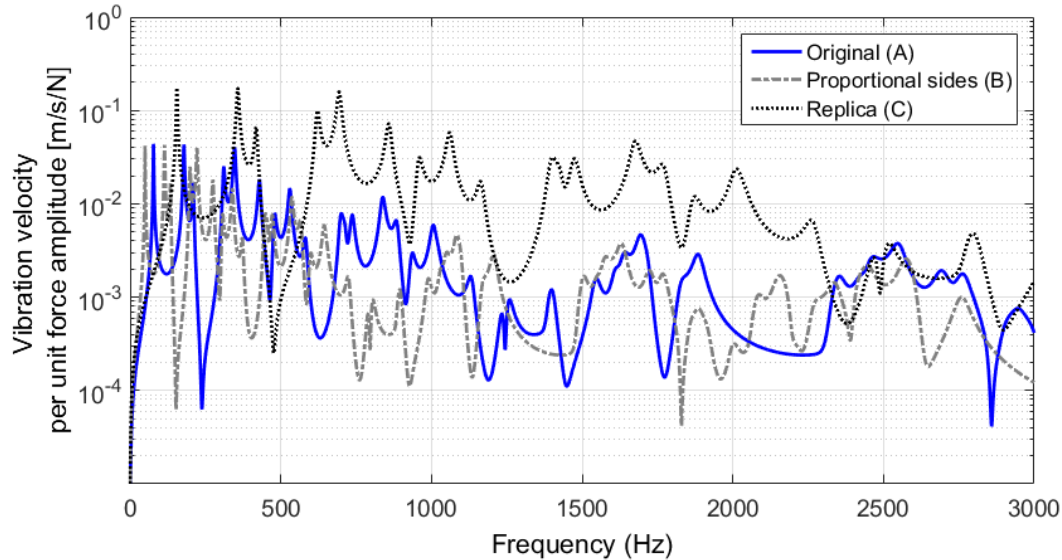


Fig. 2 Theoretical mobility function for the three considered plates at the dimensionless point of coordinates  $x = 0.4 a$  and  $y = 0.7 b$ .

## 5. Experiments

### 5.1 Experimental methods

Measurements on three panels that correspond to panels in Table 1 were conducted at Groupe d'acoustique de l'université de Sherbrooke. Each panel was placed on a weighted base and then baffled using a half inch plywood panel (4 feet by 4 feet). Figure 4 shows illustrations of the measurement setup. A vibration measurement was systematically performed before and after installation of the baffle in order to verify that it did not modify the panel response. The measurement mesh and the excitation point coordinates were treated in similitude, so as to finally have dimensionless positions. For each panel, a mechanical excitation was applied at  $x = 0.4 a$  and  $y = 0.7 b$  using a shaker. A force sensor was installed in order to monitor the force injected in the plate and then normalize the plate response by the force input. The panel vibration response was measured using a scanning laser vibrometer on a  $49 \times 43$  mesh, with regular elements of size  $1 \times 1$  cm for panel A, and  $1.25 \times 1.25$  cm for panel B. The radiated sound intensity from the panel was measured at a distance 10 cm from the panel surface using a sound intensity probe composed of two 1/2 in. microphones and a 12 mm spacer. The corresponding radiated acoustic power was estimated by multiplying the mean sound intensity by the considered panel area. A microphone array was also installed for measuring the radiated sound pressure but was used at a post-processing step. Pictures of measurements are provided in Figure 4.

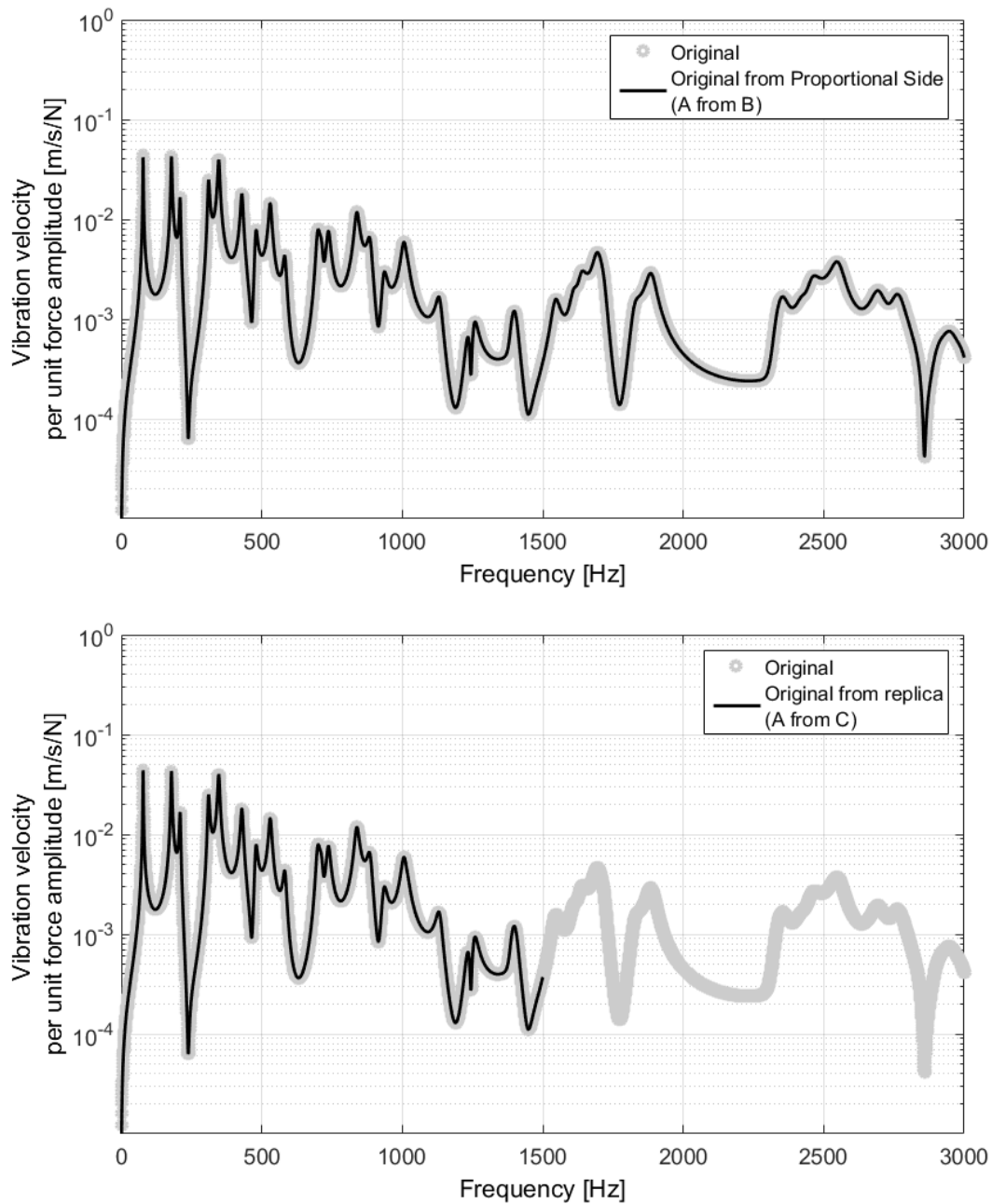


Fig. 3 Upper graph: Mobility function for panel A (original) and calculated mobility function from similitude laws and mobility function of panel B - Lower graph : Mobility function for panel A (original) and calculated mobility function from similitude laws and mobility function of panel C.



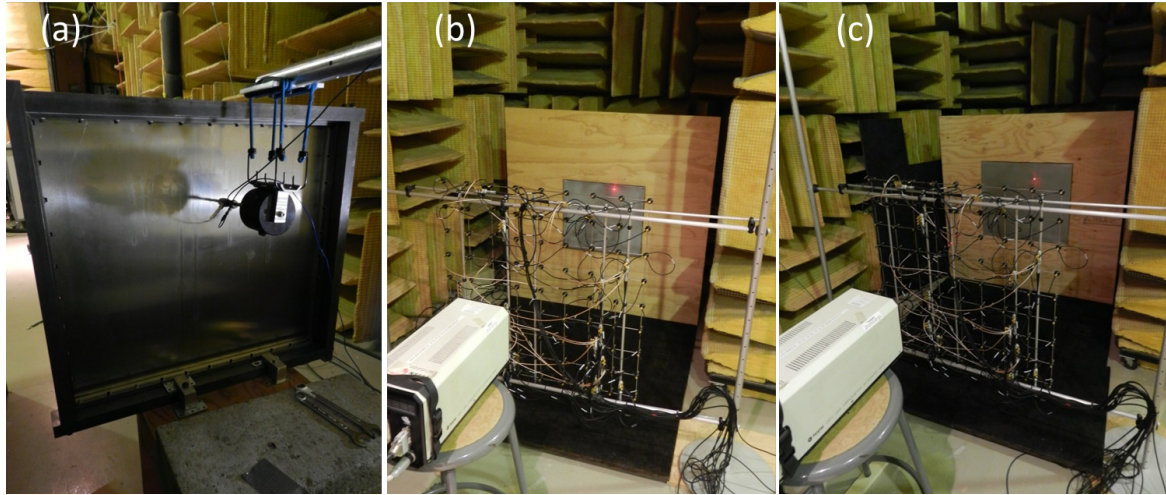


Fig. 4 Pictures of measurements: (a) Shaker installed on the back of panel B - (b) Measurement setup for panel A - (c) Measurement setup for panel B - Illustration adapted from (14).

Table 2 Summary of vibration response scaling applied to the three tested panels with corresponding figures.

Target	Scaling direction	Figure
Original plate	From proportional sides	7 (upper)
Original plate	From replica	7 (lower)
Proportional side plate	From original	8 (upper)
Proportional side plate	From replica	8 (lower)
Replica plate	From original	9 (upper)
Replica plate	From proportional sides	9 (lower)

## 5.2 Experimental results

### 5.2.1 Vibration response

All possible combinations among the three tested panels (obtain A from B, obtain B from A, etc.) have been investigated and reported in this section. Other analytical and experimental results can be found in (14, 15).

Firstly, the theoretical natural frequencies versus measured natural frequencies are presented in Figure 5 for the three tested plates and show a satisfactory agreement. Figure 6 then presents unscaled results for the three plates in terms of absolute mean vibration velocity (*i.e.* spatially averaged) normalized by input force. The vibration response of the plates appears quite different, in terms of frequency distribution and also in terms of magnitude. Figures 7, 8 and 9 finally present scaled results using all possible scaling directions, that are summarized in Table 2.

When the scaling procedure is applied to recover the original (A) or proportional sides (B) plate, the prediction of panel A from B (or the contrary) provides overall good agreement in

terms of frequency and amplitude response. The use of the replica plate provides satisfactory results that are limited in the frequency domain (up to a frequency of 500 Hz), with large amplitude errors above this frequency. This is mainly attributed to the fact that constant structural loss factor is assumed in the procedure, whereas plate C has overall larger damping than the two other plates (see spatially averaged mobility functions in Figure 6). This is attributed to the overall smaller size of panel C (panel A's length, width and thickness all divided by a factor 2), while panel B is 'a panel A extended by a 1.25 factor for length and width only'. Using the procedure described in (12), the gluing of panels A and B is made on a similar thickness while gluing of panel C is made on a thickness two times smaller which seems to influence the value of the structural loss factor finally obtained. A possibility for taking into account this variability would be not keeping the assumption of constant structural loss factor (i.e.  $r_\eta = 1$ ), but rather including a variable scaling parameter  $r_\eta$ . This will be handled in future works.

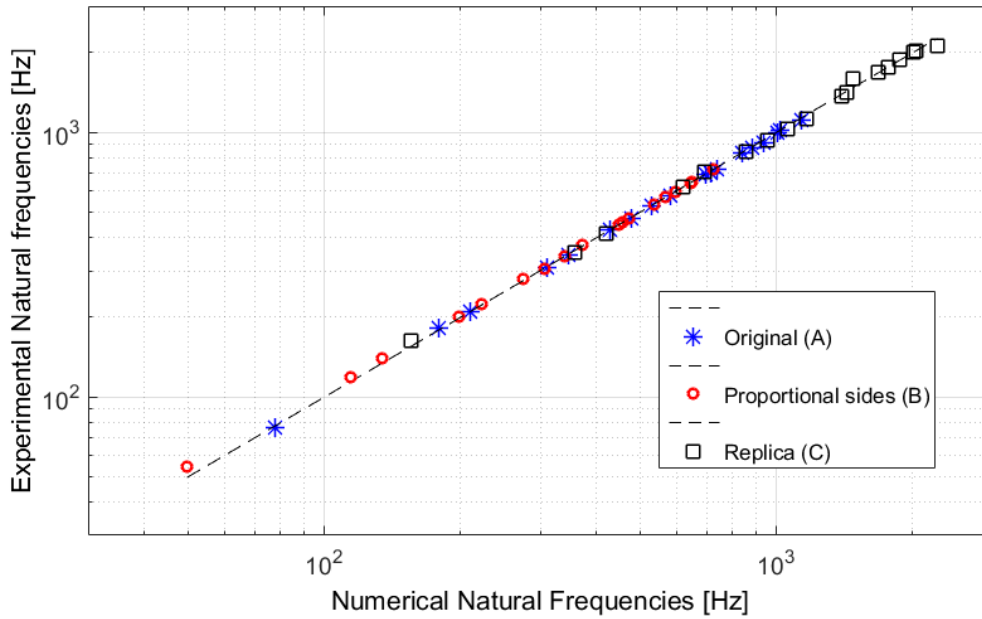


Fig. 5 Theoretical natural frequencies versus measured resonance frequencies of the three tested aluminum panels

A similar limitation is seen when the replica plate vibration response is calculated from the original plate or from the proportional side plate (see Fig.9). The natural frequencies are well scaled up to a frequency of 1000 Hz, but with amplitude errors that become very large above this frequency. The difference in structural loss factor is again considered as the main source of error in the scaling procedure. Other sources of errors can be attributed to the effects of the shaker and force sensor loading (local mass and possible additional structural damping, again supposed to be identical between cases) and to slight inaccuracies in the dimensionless positions of the excitation and measurement mesh.

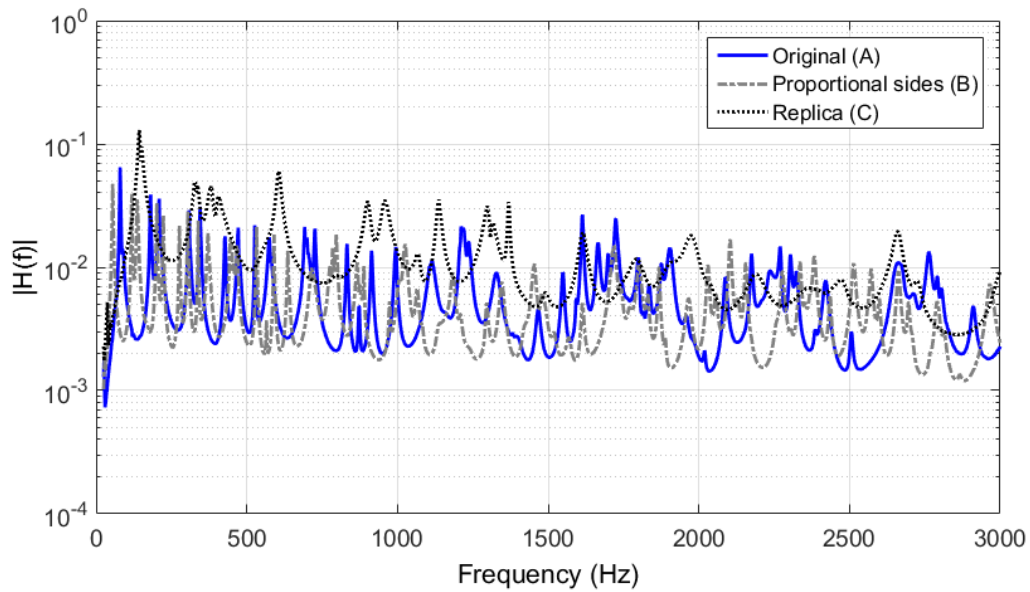


Fig. 6 Modulus of the spatially averaged mobility function for the three considered plates

5.2.2 Acoustic radiation

As for previous section, Figures 10, 11 and 12 present sound intensity scaling results using all possible scaling directions, that are summarized in Table 3. Sound intensity is preferred to sound power for presenting the results since the normalization by each plate area helps providing a direct comparison (dB values are calculated using a  $1 \times 10^{-12}$  W/m<sup>2</sup> reference). Note that the noisier behavior in presented results can be explained by the fact that calculations were made using a larger frequency step, but also because vibration response results were spatially averaged. The whole frequency range is considered in the case of figure 10, while results presented in Figs. 11 and 12 were arbitrarily limited to an upper frequency of 1000 Hz to simplify and reduce calculations.

The obtained results are in line with those presented in the previous section. When the scaling procedure is applied to recover the original (A) or proportional sides (B) plate, the prediction of panel A from B (or the contrary) provides overall good agreement in terms of frequency and amplitude response. The prediction of the replica (C) from plates A and B appears to be the most challenging, but the case of the sound intensity scaling appears to be less sensitive to the scaling direction than seen in the previous section. Even if errors in terms of magnitude and frequency are present, the overall trend of scaled results is satisfactory and could be extended to high frequency predictions base on statistical energy analysis as an example.

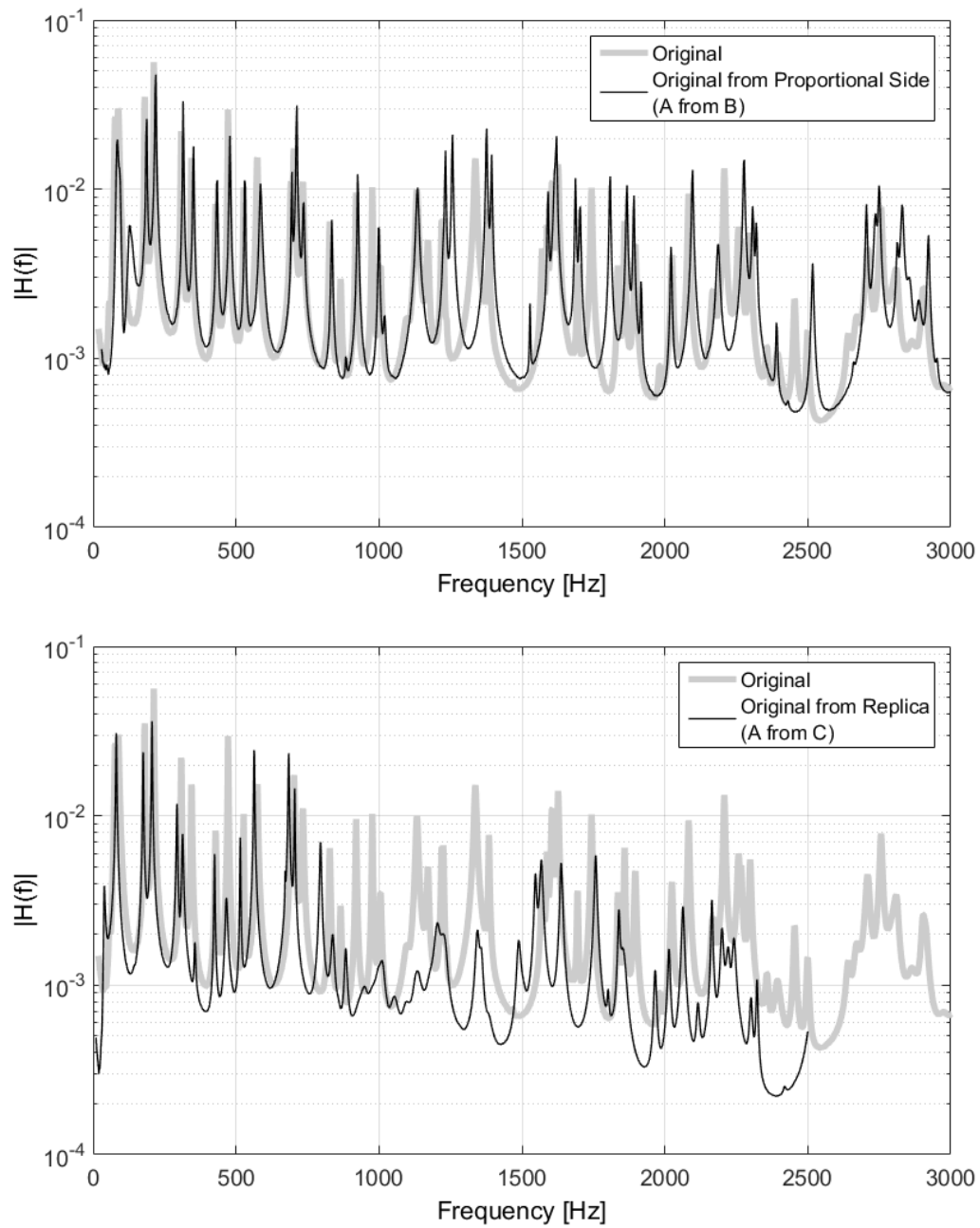


Fig. 7 Result of scaling the original plate from the proportional side plate (upper part) and from the replica plate (lower part).

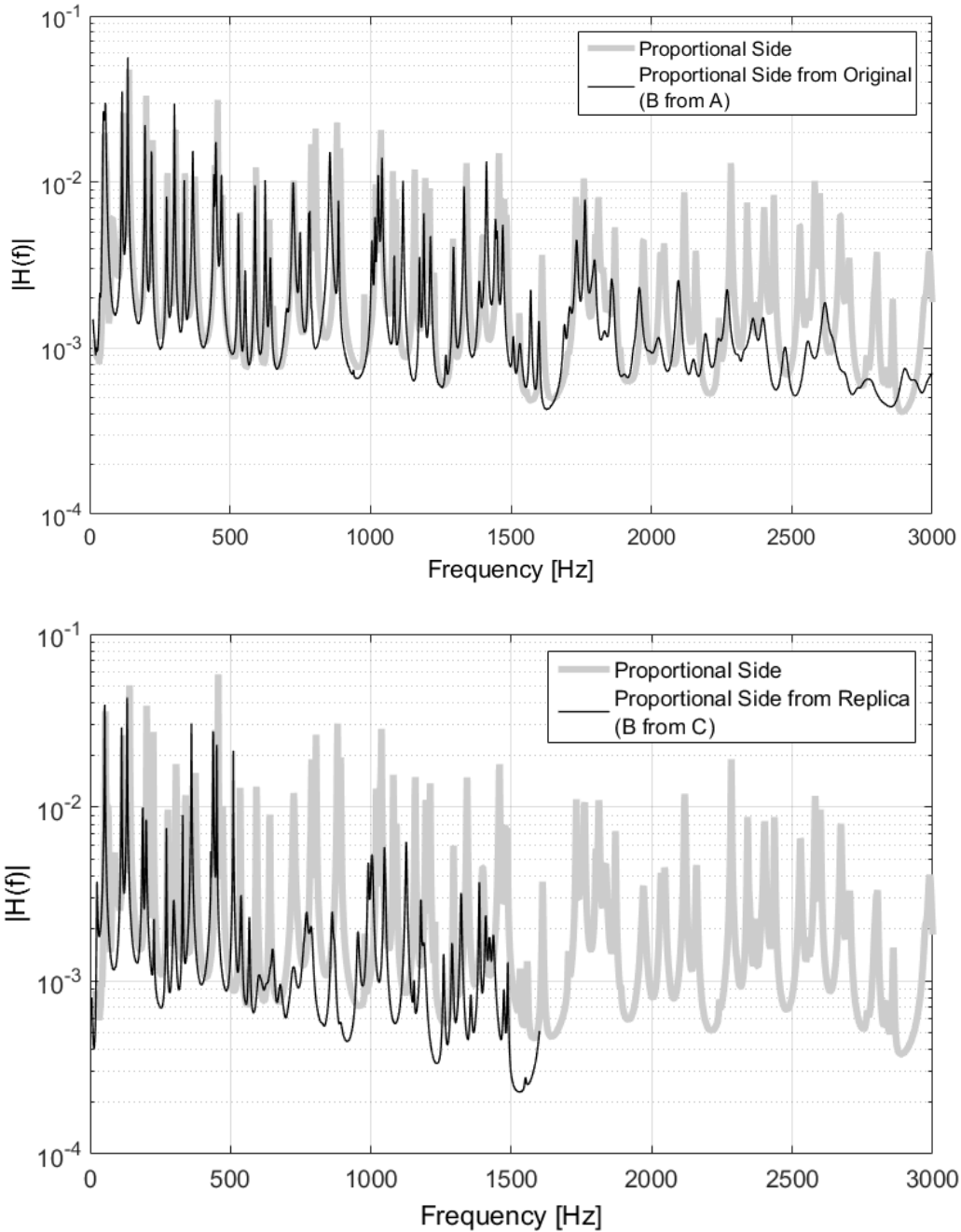


Fig. 8 Result of scaling the proportional plate from the original plate (upper part) and from the replica plate (lower part)

## 6. Conclusions

This communication investigated exact and distorted similitudes and the related scaling laws for the analysis of both dynamic response and radiated power of rectangular plates.

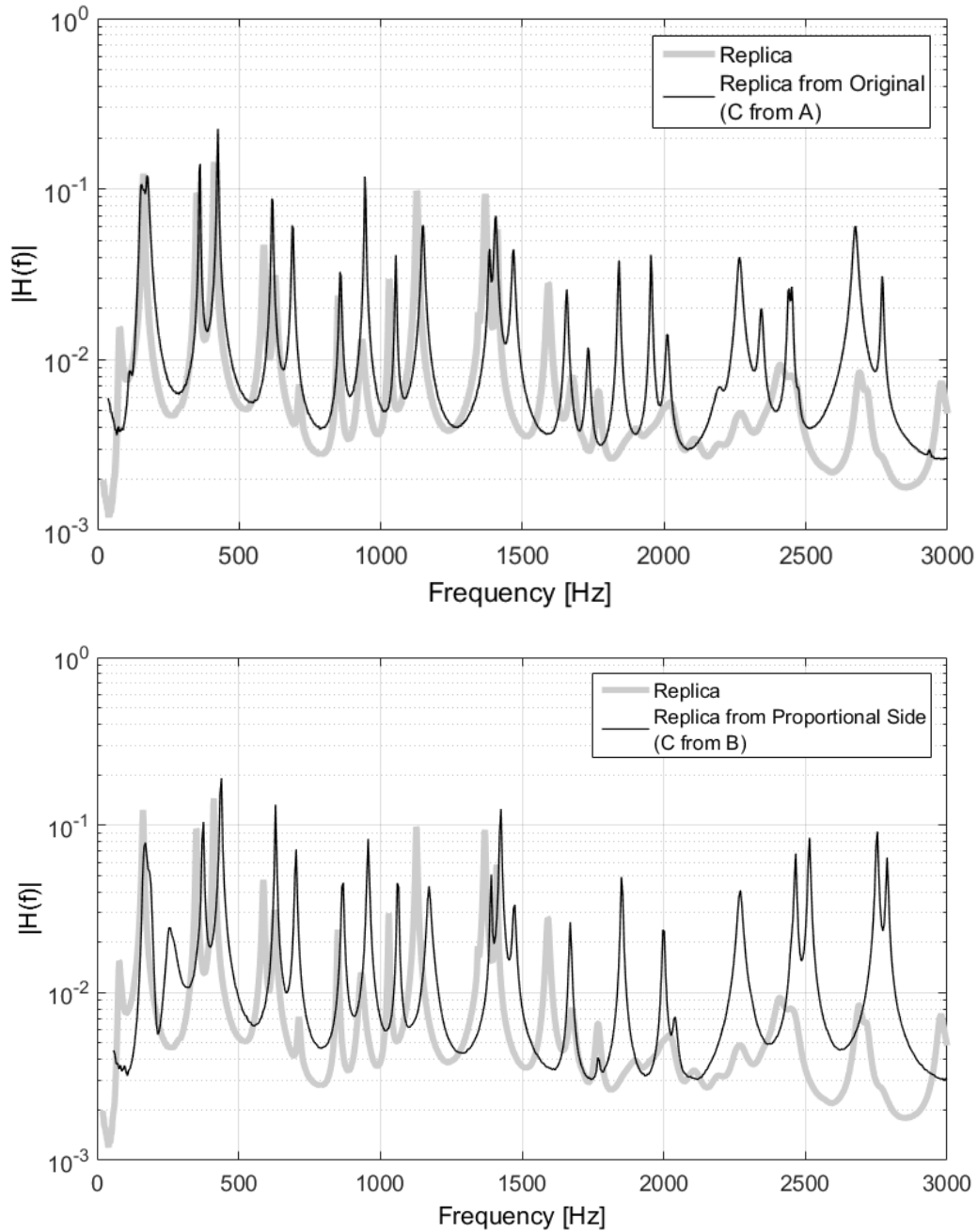


Fig. 9 Result of scaling the replica plate from the original plate (upper part) and from the proportional side plate (lower part)

Emphasis was put on reporting a comprehensive comparison of possible scaling directions that can be followed. The obtained results in the experimental part of this work show

Table 3 Summary of sound intensity scaling applied to the three tested panels with corresponding figures numbers.

Target	Scaling direction	Figure
Original plate	From proportional sides	10 (upper)
Original plate	From replica	10 (lower)
Proportional side plate	From original	11 (upper)
Proportional side plate	From replica	11 (lower)
Replica plate	From original	12 (upper)
Replica plate	From proportional sides	12 (lower)

that under the assumption of constant loss factor, the prediction of a proportional side plate seems to be the most promising methodology. The modification of thickness with a replica plate limits the highest frequency that can be reached using the scaling procedure, and the prediction of other plates response using a scaled-down replica is identified as the most challenging case within the presented ones. This indicates that the procedure could be especially suited for testing smaller samples than final ones (*i.e.* a smaller panel than the actual one with same thickness) with promising implications in laboratory testing when facilities usually have size or space limitations. Interestingly, the radiated sound power (or sound intensity) can be quite well estimated using parent models even if the corresponding structural response is not perfectly reconstructed. A next step would be to couple the scaled acoustic response with enclosures, as was already proposed in (10, 11).

**References**

[1] Chambers, J.R. (2009), Modeling flight : the role of dynamically scaled free-flight models in support of NASAs aerospace programs, NASA SP 2009-575.

[2] Coutinho, C.P., Baptista, A.J. and Rodrigues, J.D. (2016), "Reduced scale models based on similitude theory: A review up to 2015", *Eng. Struct.*, 119, 81-94. <https://doi.org/10.1016/j.engstruct.2016.04.016>.

[3] Asl, M.E., Niezrecki, C., Sherwood, J. and Avitabile, P. (2015), Predicting the vibration response in sub-component testing of wind turbine blades, *Proceedings of the 33rd IMAC a Conference and Exposition on Structural Dynamics*, Orlando, Florida, February.

[4] Rezaeepazhand, J. and Simites, G.J. (1996) "Design of scaled down models for predicting shell vibration response", *J. Sound Vib.*, 195(2), 301-311. <https://doi.org/10.1006/jsvi.1996.0423>.

[5] Wu, J.J. (2003), "The complete-similitude scale models for predicting the vibration characteristics of the elastically restrained flat plates subjected to dynamic loads", *J. Sound Vib.*, 268(5), 1041-1053. [https://doi.org/10.1016/S0022-460X\(03\)00303-1](https://doi.org/10.1016/S0022-460X(03)00303-1).

[6] Singhatanadgid, P. and Songkhla, A.N. (2008), An experimental investigation into the use of scaling laws for predicting vibration responses of rectangular thin plates. *J. Sound Vib.*, 311(1),314-327, 2008. <https://doi.org/10.1016/j.jsv.2007.09.006>.

[7] De Rosa, S., Franco, F., and Polito, T. (2011) Structural similitudes for the dynamic response of plates and assemblies of plates. *Mechanical Systems and Signal Processing*, 25(3):969–980.

[8] De Rosa, S., Franco, F., and Meruane, V. (2015) Similitudes for the structural response of

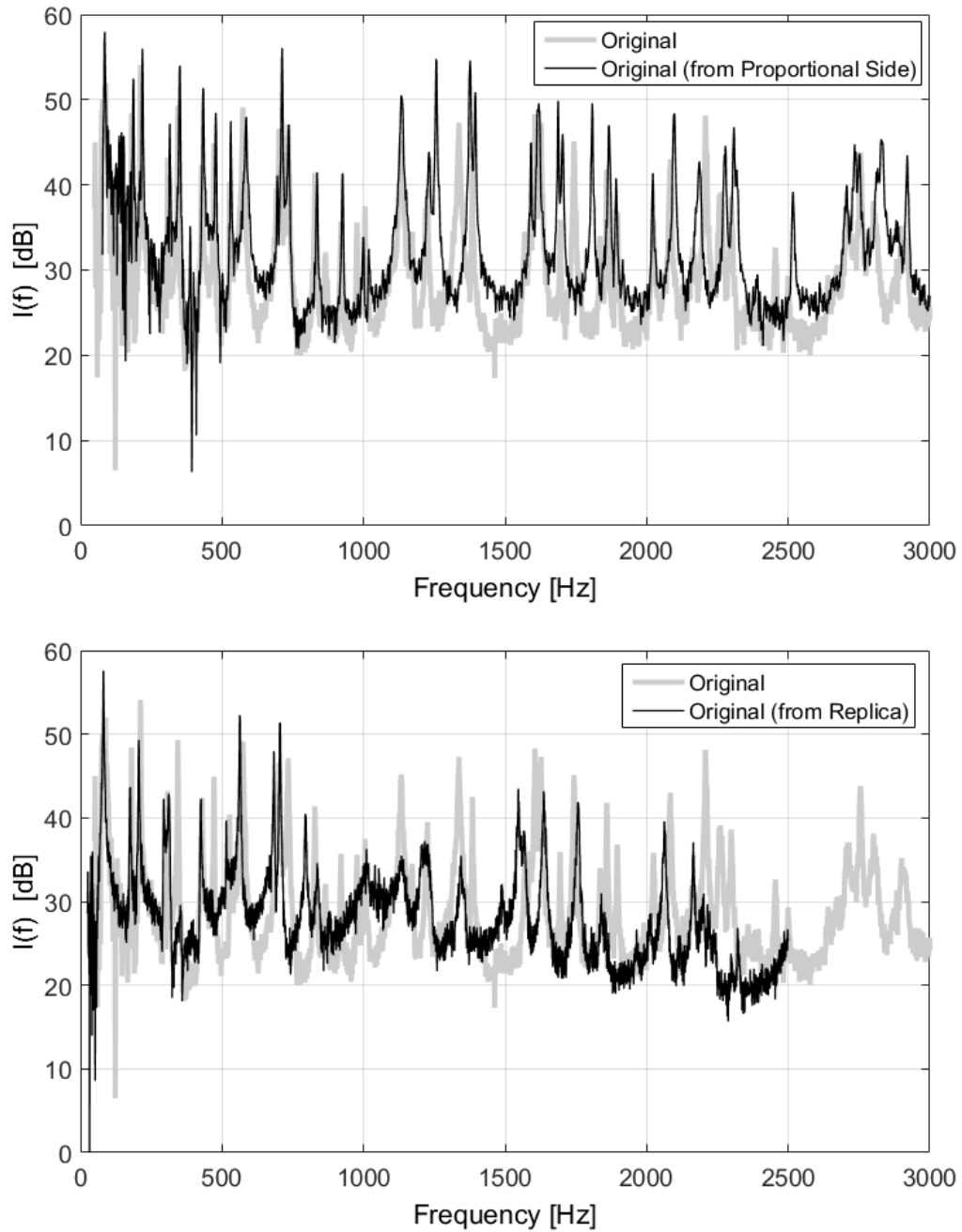


Fig. 10 Sound intensity : Result of scaling the original plate from the proportional side plate (upper part) and from the replica plate (lower part).

flexural plates. *Proceedings of the Institution of Mechanical Engineers, Part C - Journal of Mechanical Engineering Science*, 230(2):174–188.



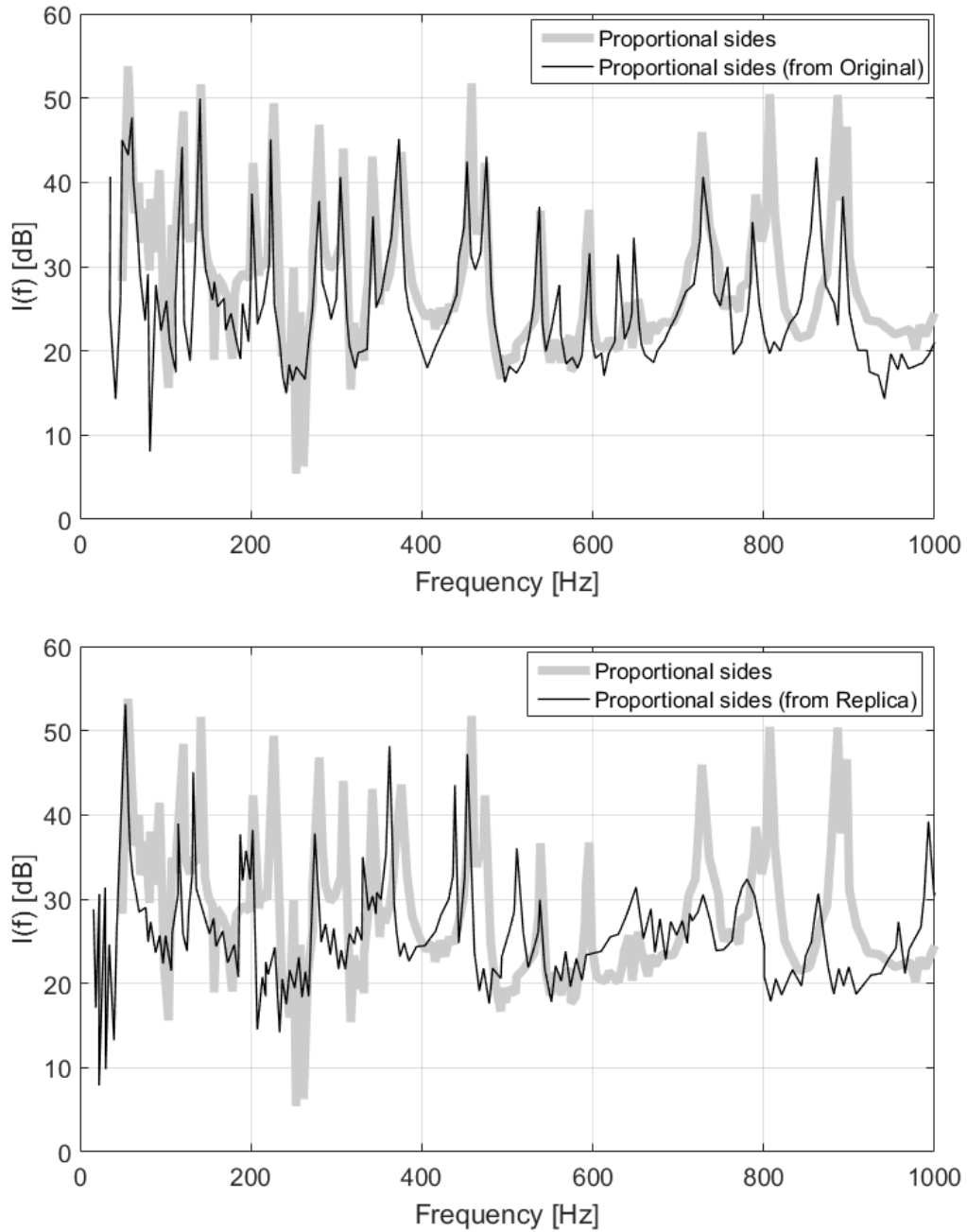


Fig. 11 Sound intensity : Result of scaling the proportional side plate from the original plate (upper part) and from the replica plate (lower part).

- [9] Meruane, V., De Rosa, S., and Franco, F. (2015) Investigations into the use of exact and distorted similitudes for the frequency response of plates. In *NOVEM (NOise and Vibration - EMerging*

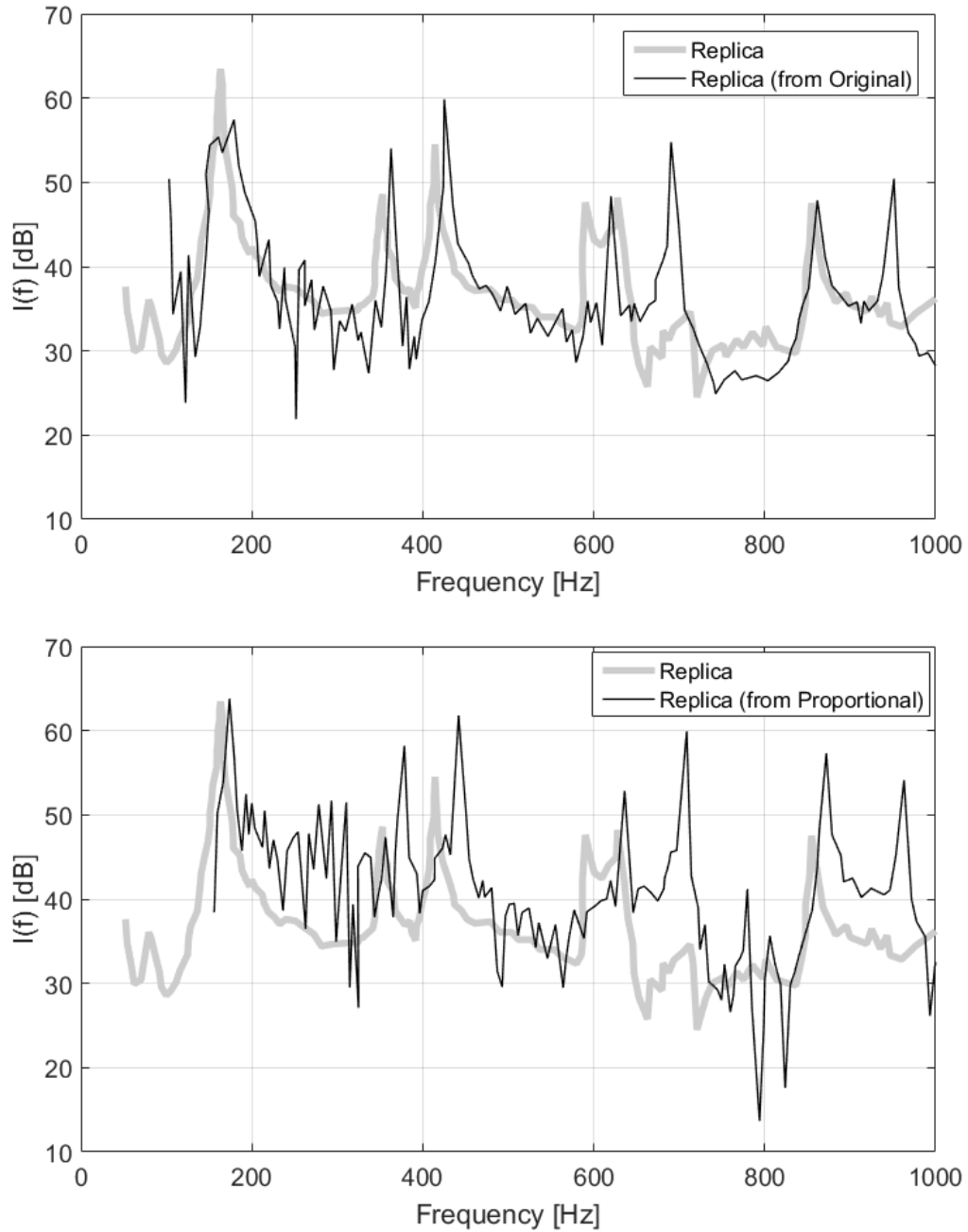


Fig. 12 Sound intensity : Result of scaling the replica plate from the original plate (upper part) and from the proportional side plate (lower part).

*technologies*), Dubrovnik, Croatia, April 13-15.

[10] Cheng, L. and Lesueur, C. (1990) Preliminary study on vibroacoustic model scaling of a structure

coupled to an acoustic cavity. *Journal d'Acoustique*, 3:349–359.

- [11] De Rosa, S., Franco, F., Li, X., and Polito, T. (2012), A similitude for structural acoustic enclosures. *Mechanical Systems and Signal Processing*, 30:330–342.
- [12] Robin, O., Chazot, J.-D., Boulandet, R., Michau, M., Berry, A. and N. Atalla, N. (2016), A plane and thin panel with representative simply supported boundary conditions for laboratory vibroacoustic tests. *Acta Acust. united Ac.*, 102 (1):170–182.
- [13] Elliott, S.J., and Johnson, M.E. (1993), Radiation modes and the active control of sound power. *J. Acoust. Soc. Am.*, 94(4):2194–2204.
- [14] Robin, O., De Rosa, S., and Berry, A. (2016), Similitudes for the structural response and radiated power from plates. Internoise2016 Congress, 21-24 August Hamburg, Germany, 1-10.
- [15] Margherita, P. (2016), Theoretical and experimental analyses for the vibroacoustic response of plates in similitude. Master Thesis in Aerospace Engineering, Università degli Studi di Napoli Federico II, Napoli, Italy (2016).
- [16] O. Robin, O., Franco, F., Ciappi, E., De Rosa, S., and Berry, A. (2017), Similitudes for the structural response and radiated power from plates. FLINOVIA2 Symposium, 27-28 April, Penn State University, State College, 1-16.

CC